Firefighter helmets and cervical intervertebral Kinematics: An OpenSim-Based biomechanical study

Gustavo M. Paulon [a], S. Sudeesh [b], Leonardo H. Wei [c], Suman K. Chowdhury [a,*]

[a] *Department of Industrial and Systems Engineering, University of Florida, Gainesville, FL, USA*
[b] *Department of Physical Medicine and Rehabilitation, Northwestern University, Chicago, IL, USA*
[c] *Department of Industrial, Manufacturing, and Systems Engineering, Texas Tech University, Lubbock, TX, USA*

ABSTRACT

The assessment of cervical intervertebral kinematics can serve as the basis for understanding any degenerative changes in the cervical spine due to the prolonged wear of a heavyweight, imbalanced firefighting helmet. Therefore, this study aimed to analyze cervical intervertebral kinematics using the OpenSim musculoskeletal modeling platform in order to provide much-needed insights into how the inertial properties of firefighter helmets affect cervical spinal mobility. A total of 36 firefighters (18 males and 18 females) were recruited to perform static and dynamic neck flexion, extension, and left and right lateral bending tasks for three conditions: 1) no-helmet, 2) US-style helmet with a comparatively superior center of mass (COM), and 3) European-style helmet with relatively higher mass but an inferior COM. Three custom-made OpenSim head-neck models were created to calculate cervical intervertebral kinematics for each helmet condition. Results showed that helmet use significantly (p < 0.001) affects neck and cervical spinal kinematics. Despite its lighter weight, the superior COM placement in the US-style helmet caused more pronounced angular changes and higher velocity of peak flexion and extension angles compared to the European-style helmet across all cervical joints. Moreover, results revealed discrepancies between OpenSim-derived neck and cervical range-of-motion and those reported in previous in-vivo studies. In conclusion, the present study underscores the importance of designing firefighter helmets with a lower profile (less superior COM) to enhance neck range of motion and minimize potential neck injuries.

1. Introduction

Neck pain is a multifactorial musculoskeletal health condition with a high global prevalence. According to the 2019 Global Burden of Disease (GBD) Study, neck pain was among the top four most prevalent musculoskeletal disorders (MSDs) and affected 222.7 million people (2.9 % of total population) worldwide (GBD, 2019). Various factors, ranging from ergonomic factors in the workplace to daily lifestyle and recreational activities, contribute to the onset and persistence of neck pain. For instances, prolonged static postures (Christensen et al., 2023), repetitive neck motions (Guidotti, 1992), heavy lifting or working in awkward neck postures (Ariens et al., 2000), sedentary lifestyle and poor sleep quality (Peterson and Pihlström, 2021), and chronic stress and certain mental health conditions (Kim et al., 2013) have been associated with work-related neck MSDs. In addition to these causes, the usage of helmets and other head mounted devices in medical surgery (Nimbarte et al., 2013), military (Hanks et al., 2018), firefighting (Park et al., 2014; Wang et al., 2021), sports (Kent et al., 2020), and vehicle safety applications (Diyana et al., 2019) were found to increase the likelihood of neck MSDs.

Previous biomechanical studies have primarily associated excessive weight and shifted center of mass (COM) of helmets with the risks of neck injuries. For instance, Van Dijke et al. (1993) and Newman et al. (2022) studied the influence of jet pilot helmets' inertial properties on the risk of neck injury and found that helmets significantly increase the neck joint reaction moments. Barrett et al. (2023) showed that the inertial properties (i.e., COM, mass, and moment of inertia) of a military helmet resulted in higher compressive forces in the cervical spine. Other studies on construction (Boschman et al., 2015), mining (Torma-Krajewski et al., 2006), and firefighting (Wang et al., 2021) helmets also emphasized the importance of enhancing the ergonomic aspects (i.e., inertial properties) of helmets in order to reduce neck discomfort and MSDs. Among them, firefighter helmets are usually heavier than other helmet types because they include two shells and other padding

* Corresponding author at: Department of Industrial and Systems Engineering, University of Florida, 417 Weil Hall, Gainesville, FL, 32603, Florida, USA.
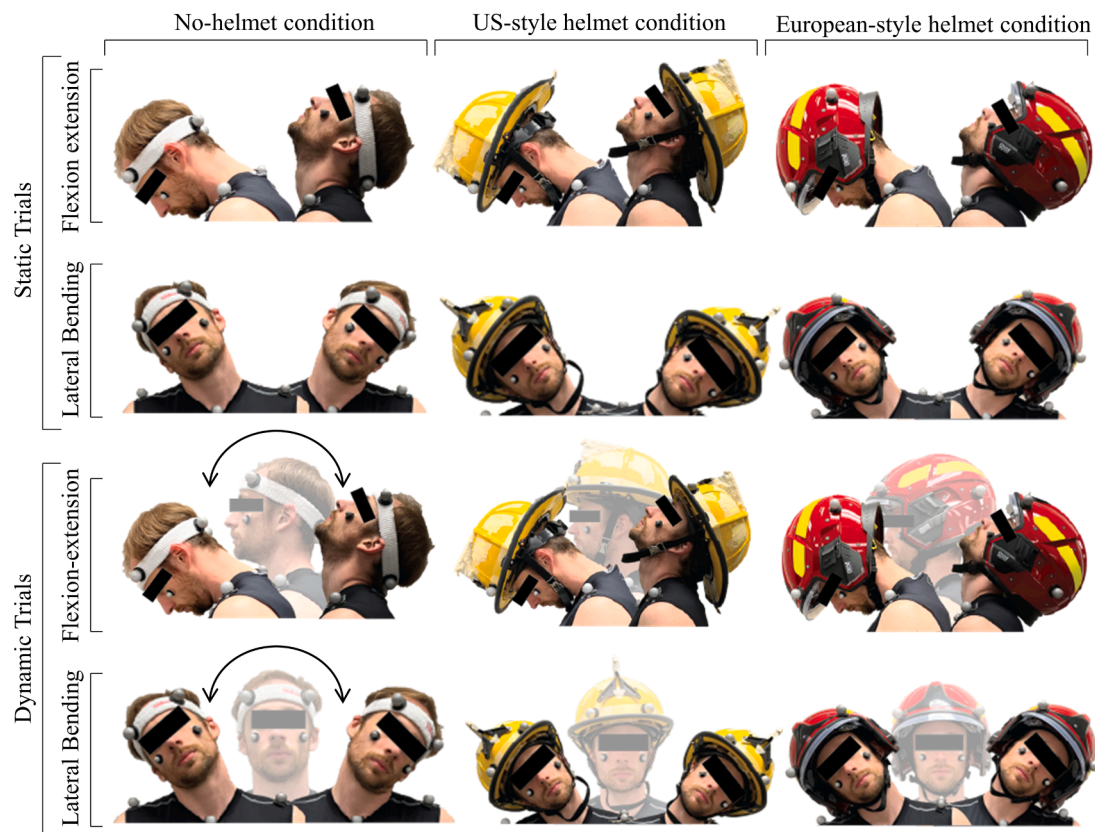 *E-mail address:* sk.chowdhury@ufl.edu (S.K. Chowdhury).

Fig. 1. A schematic presentation of (a) Task 1 wherein subjects performing static flexion, extension, left, and right bending tasks and (b) Task 2, in which they performed dynamic flexion–extension and dynamic lateral bending tasks. Both tasks were performed for three different conditions: 1) baseline, no-helmet (left), 2) US-style helmet (middle), and 3) European-style helmet (right) in a random order.

materials to provide high flame and impact protection to the users. Additionally, the modern firefighter helmets include other supporting accessories, such as face-shield, visor, and lighting equipment. Their additions can further increase the likelihood of cervical spinal injuries due to the increase in the total helmet weight and a potential shift of the helmet COM. Especially, these changes can make female users more vulnerable to neck pain as they have weaker neck muscles (Vasavada et al., 2008) and smaller cervical vertebra (Stemper et al., 2008) than males. It was also reported that about 23 % of all firefighter injuries (27,150 cases out of 118,070 cases) are related to the head, neck, and shoulder – out of which, 5.5 % involved strains or overexertion on the head and neck (Campbell and Molis, 2022). As firefighter helmets are worn daily for a prolonged duration, their repetitive usage over time can result in degenerative neck injuries, such as spinal cord spondylosis, degenerative disc diseases, and ossification of the ligamentum flavum (Echarri and Forriol, 2005).

As indicated in previous clinical (Hino et al., 1999; Hirsch et al., 1967) and biomechanical (Panjabi et al., 2001) studies, the assessment of cervical intervertebral kinematics can be used as surrogate measures of degenerative changes occurring in the cervical spine because these changes can adversely affect the neck joint mobility. Thus, an accurate information about the cervical intervertebral joint mobility under the effects of no-helmet and helmet conditions can serve as the basis to evaluate how the helmet inertial properties may cause abnormal neck conditions. A number of in-vivo experimental studies using dynamic fluoroscopic system (Zhou et al., 2020), dynamic stereo-radiographic system (Anderst et al., 2015), and three-dimensional MRI (Ishii et al., 2006) have reported neck and cervical intervertebral ROM. As these in-vivo studies are labor-, time-, and technology-intensive, a handful of studies used in-silico methods, such as OpenSim (an open-source musculoskeletal modeling platform) (Barrett et al., 2022a; Barrett

et al., 2022b; Mathys and Ferguson, 2012; Newman et al., 2022) because of their non-invasiveness nature and ease-of-use in modeling the head-helmet dynamics. Nevertheless, they overlooked the influence of helmet on cervical intervertebral kinematics, especially during dynamic neck movements. Additionally, our systematic literature review showed only one survey-based study on the firefighter helmet by Wang et al. (2021). They reported that a poorly-fitting, imbalanced helmet can restrict firefighter's neck mobility, which motivated us to conduct a thorough biomechanical investigation to assess the impacts of firefighter helmets on cervical intervertebral kinematics—the potential surrogate measures of degenerative neck injuries.

Two types of helmets (Figure 01) are frequently used by firefighters: 1) US-style helmets (resemblance to hats) and 2) European-style helmets (resemblance to aviation helmets). There has been an ongoing effort to popularize European-helmet among US firefighters for its competitive advantages, such as 1) its inferior COM (low profile), 2) the helmet shell provides coverage of the occipital and temporal skull regions, and 3) its brim-less shape allows firefighters to access narrow aisles. In contrast, the US-style helmet is lighter in weight and has a superior COM (high profile) compared to the European-style helmet. In this study, we tested the biomechanical impact of the inertial properties of each helmet type in terms of cervical intervertebral kinematics. Therefore, this study aimed to investigate the effects of firefighter helmet inertial properties on neck and cervical intervertebral kinematics, especially during various neck dynamic movements. We hypothesized that a helmet with higher mass and superior COM from C0-C1 joint would more adversely affect the total neck angle and individual cervical joint kinematics, particularly among female users, compared to a helmet with lesser weight and a COM less offset from C0-C1 joint. A quantitative analysis of their inertial properties and how their variations affect cervical intervertebral kinematics would provide an unprecedented understanding of firefighter's

Table 1

Inertial properties (mass, center of mass, and moment of inertial) of US-style and European-style helmets. X, Y, and Z respectively indicate anterior-posterior, inferior-superior, and medio-lateral directions. A positive value refers to anterior, right lateral, and superior directions. The center of mass was calculated with respect to the C0-C1 joint[1].

	Mass (kg)	Center of Mass (m)			Moment of Inertia (kg.m2)			Moment of Inertia combined with the head (kg.m2)		
		X	Y	Z	Ixx	Iyy	Izz	Ixx	Iyy	Izz
US-style helmet	1.77	0.002	0.152	−0.006	0.017	0.028	0.022	0.092	0.088	0.10
European-style helmet	2.02	0.019	0.094	−0.008	0.023	0.03	0.031	0.076	0.068	0.090

[1] The center of rotation of the C0-C1 joint is located at the point (X Y Z) = (0.04335 m, 0.015 m, 0 m) from the origin of the C1 body of the MASI model.

neck MSD mechanisms and assist practitioners to design an injury-mitigating firefighter helmet that can be worn for prolonged time.

2. Methods

2.1. Participants

We recruited eighteen male (weight: 88.5 ± 18.9 kg; height: 1.77 ± 0.09 m; BMI: 28.8 ± 5.39; Age: 39.2 ± 7.23 years) and eighteen female (weight: 69.5 ± 12.2 kg; height: 1.64 ± 0.05 m; BMI: 24.2 ± 2.85; Age: 31.2 ± 8.62 years) firefighters from the local fire departments. The inclusion criteria required all participants to be healthy and did not have any recent history of neck, shoulder, and back injury. Prior to their participation, they signed an informed consent form approved by the local Institutional Review Board (IRB2020-708).

2.2. Experiment

Participants primarily performed two repetitions of static task—holding a static head-neck position in full flexion, extension, and left and right lateral bending for five seconds—and two repetitions of dynamic neck ROM task. The pace of the flexion–extension and left--right lateral ROM tasks were controlled using three beat sounds (i.e., three seconds) of a digital metronome. Each of these tasks were
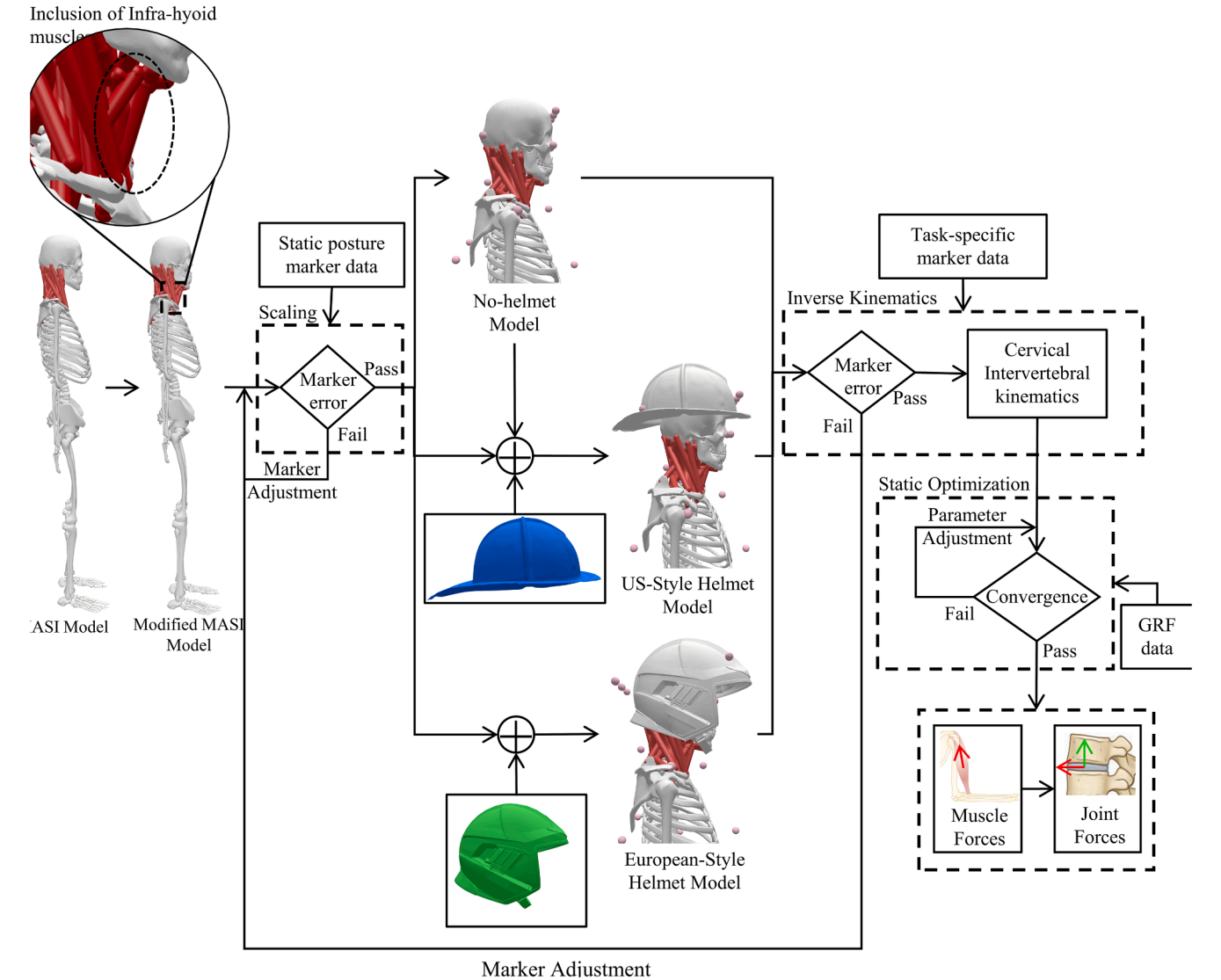

Fig. 2. OpenSim inverse-solution workflow displaying the development of three modified MASI models: 1) no-helmet, 2) US-style helmet, and 3) European-style helmet conditions and their inverse simulation pipelines to calculate task-specific neck and cervical kinematics using experimental data.

Table 2

Neutral and peak flexion, extension, right bending, and left bending neck angles (C0-T1) while holding static neck postures and performing dynamic neck movements. Negative values correspond to a flexed neutral angle while positive values correspond to an extended posture.

		Static neck posture		Dynamic neck movement	
Peak Flexion (°)	No Helmet	Male: 40.8 ± 2.14 Female: 50.4 ± 1.23	45.6 ± 2.02	Male: 43.0 ± 1.75 Female: 48.7 ± 1.44	45.8 ± 1.69
	US-style Helmet	Male: 50.5 ± 0.88 Female: 54.4 ± 0.89	52.5 ± 0.98	Male: 49.9 ± 1.17 Female: 50.7 ± 1.10	50.3 ± 1.11
	European-style Helmet	Male: 47.6 ± 1.33 Female: 51.3 ± 1.51	49.4 ± 1.45	Male: 46.5 ± 1.63 Female: 49.8 ± 1.52	48.1 ± 1.58
Peak Extension (°)	No Helmet	Male: 57.4 ± 2.19 Female: 64.9 ± 1.78	61.2 ± 2.12	Male: 55.3 ± 2.87 Female: 60.0 ± 2.71	57.7 ± 2.77
	US-style Helmet	Male: 51.9 ± 3.06 Female: 58.4 ± 1.59	55.1 ± 2.48	Male: 50.4 ± 3.64 Female: 46.6 ± 2.19	48.5 ± 2.95
	European-style Helmet	Male: 56.4 ± 3.10 Female: 63.2 ± 1.69	59.8 ± 2.55	Male: 53.1 ± 3.13 Female: 57.9 ± 1.73	55.5 ± 2.52
Peak Right Bending (°)	No Helmet	Male: 34.3 ± 1.39 Female: 39.3 ± 0.88	36.8 ± 1.27	Male: 36.1 ± 1.16 Female: 41.3 ± 1.37	38.7 ± 1.37
	US-style Helmet	Male: 39.1 ± 0.71 Female: 41.4 ± 0.68	40.2 ± 0.72	Male: 39.1 ± 0.76 Female: 39.0 ± 0.69	39.0 ± 0.71
	European-style Helmet	Male: 36.8 ± 1.05 Female: 38.4 ± 0.58	37.6 ± 0.85	Male: 36.2 ± 0.90 Female: 38.3 ± 0.62	37.3 ± 0.79
Peak Left Bending (°)	No Helmet	Male: 33.6 ± 1.26 Female: 38.1 ± 0.90	35.9 ± 1.19	Male: 33.5 ± 2.33 Female: 40.2 ± 1.32	36.8 ± 2.00
	US-style Helmet	Male: 38.0 ± 0.82 Female: 41.8 ± 0.63	39.9 ± 0.84	Male: 37.8 ± 1.30 Female: 41.1 ± 0.48	39.4 ± 1.03
	European-style Helmet	Male: 36.7 ± 0.87 Female: 38.3 ± 0.54	37.5 ± 0.73	Male: 34.0 ± 1.81 Female: 38.1 ± 0.50	36.0 ± 1.37
Neutral Posture (°)	No Helmet	Male: 7.01 ± 9.00 Female: 7.88 ± 7.15	7.45 ± 7.92		
	US-style Helmet	Male: 0.27 ± 11.6	−1.00 ± 9.52		

randomly repeated for three different helmet conditions: 1) baseline, no-helmet, 2) US-style helmet (Bullard UM6WH), and 3) European-style (Cairns XF1) helmet in a random order (Fig. 1). To ensure that participants obtained their maximum ROM, they were asked to fully flex their head forward and downward towards the chest during flexion tasks, fully extend their head backward while looking as far upward as possible during the extension tasks and bent their head laterally as much as possible for right and left bending. The National Fire Protection Association (NFPA) standards require firefighters to securely tighten the helmet using a retention system and chin strap to ensure that there is no relative movement between the helmet and the head. We collected full-body movements using a 10-camera motion capture system at 60 Hz (Krestel 1300; Motion Analysis, California, USA) and ground reaction forces using two force plates (Bertec, Ohio, USA) at 600 Hz. We also used a handheld, rotating 3D scanner (EinScan HX, Shining 3D, Hangzhou, China) to image individual helmets at 20 Hz frame rate. The kinematics data were pre-processed in Cortex-9 software (Motion Analysis Corporation, Rohnert Park, California, USA). Though we used full-body plug-in gait marker set (Vicon, 2023) consisting of 44 markers in the experimental protocol, we created additional 32 virtual markers in Cortex to measure link-segment anthropometric measures accurately. The force plate data were exported from Cortex-9 as C3D format and then converted to motion (.mot) files using C3Dtools (Mokhtarzadeh and Bagheri, 2023) in order to input them into OpenSim.

2.3. OpenSim modeling

The MASI (Musculoskeletal model for the Analysis of Spinal Injury) model, a validated full-body model developed by Cazzola et al. (2017), was used as a base model for our study. Then, we added infra-hyoid muscles to the base model—taken from HYOID model (Mortensen et al., 2018)—to achieve more biofidelic cervical intervertebral kinetic results. The modified model included 35 rigid body segments, 34 body joints, 23 torque actuators, 98 Hill's type neck muscles, and inherited head and neck models of Vasavada et al. (1998) that implements three rotational (roll, pitch, and yaw) degrees of freedom (DoF) to each cervical joint, dividing the cervical spine in two different kinematic chains—from C7-T1 (independent) to C2-C3 and from C1-C2 (independent) to C0-C1—and calculating the kinematics of the chain based on the estimated kinematics of the independent coordinates.

Three different versions of our modified model—a no-helmet, a US-style helmet, and a European-style helmet model—were created. Prior to the creation of head-helmet OpenSim interfacing, the geometrical shape of each helmet type was created in NMSBuilder (Valente et al., 2017) software and their inertial properties (Table 1) were estimated in ANSA (BETA CAE Systems SA, Greece) finite element pre-processor platform. It was observed that the COM of the US-style helmet is 5.8 cm superior and 1.7 cm posterior than the European-style helmet. However, the European-style helmet was 250 g heavier than the US-style helmet. As the helmet was securely tightened with the head, and the axis of rotation of the total skull is C1 (the occiput, C0, of the total skull, sits on C1), we considered the C0-C1 joint to calculate the joint MOI of the head and helmet.

2.4. OpenSim simulation

Though we controlled the pace and duration of the experimental tasks using a metronome, slight discrepancies remained across the tasks and the subjects. Therefore, we down-sampled both kinematics and force plate data to 100 data points for between-task and between-subject comparisons. In OpenSim, we implemented inverse pipelines (Fig. 2) that include subject-specific model scaling, inverse kinematics (IK), inverse dynamics (ID), and static optimization (SO) processes. We scaled (RMS:< 1 cm; maximum: < 2 cm) each custom-made OpenSim model by using marker data collected during corresponding baseline, static head-neck neutral posture for each helmet condition. In head-helmet

Table 2 (*continued*)

	Static neck posture	Dynamic neck movement
European-style Helmet	Female: −2.28 ± 7.36 Male: 2.62 ± 8.89 Female: 2.56 ± 6.49	2.59 ± 7.58

OpenSim models, we applied a welded joint to the head-helmet interface. We then used task-specific motion capture data to perform IK simulations. In some trials, adjustments were made to the model markers and their weightages in order to keep the root mean square (RMS) < 2 cm and maximum marker errors < 4 cm during the IK analysis. The IK and the ground reaction force data were then used as inputs to perform SO.

The neck angle was calculated by summing the kinematics of all cervical intervertebral joints (C0-C1 to C7-T1). The flexion–extension and lateral bending ROM of individual cervical joints and the neck was calculated by taking the difference between their maximum positive and negative angular values during respective dynamic motions. Due primarily to poor marker (pelvis and other markers of some subjects moved or fall off during the experimental tasks) data and some challenges during experimental data collection, we abled to simulate OpenSim models of a total of 24 subjects—12 males (weight: 90.6 ± 19.1 kg; height: 1.77 ± 0.066 m; BMI: 28.8 ± 2.85 kg/m^2; Age: 38.2 ± 7.97 years) and 12 females (weight: 67.4 ± 8.28 kg; height: 1.67 ± 0.055 m; BMI: 24.2 ± 2.85 kg/m^2; Age: 31.2 ± 8.62 years)—and the further analysis of this study was based on these 24 best subject's data.

2.5. Statistical Analysis

We calculated the descriptive statistics (mean and standard error) of peak flexion, peak extension, peak left bending, peak right bending, flexion–extension ROM, lateral bending ROM, and neutral posture of individual cervical intervertebral joints and the neck (C0-T1) as a whole for all static and dynamic motion trials across all subjects (males and females separately). In order to investigate the effects of helmets and sex and their interaction on neck and cervical intervertebral peak angles and ROM data, we first evaluated data normality, with Shapiro-Wills test (α < 0.05), and homoscedasticity, with Levene's test (α < 0.05), conditions. As the majority of the peak angle and neutral posture data violated these two conditions even after logarithmic, exponential, and power transformations, we employed Friedman non-parametric test wherein the effects of *helmet condition* (no-helmet, US-style helmet, and European-style helmet) and *subject* were respectively treated as fixed and randomized block variables. Additionally, we considered Kruskal-Walis non-parametric test to study the *sex* (male and female) effect. In both Kruskal-Walis and Friedman tests, peak flexion, extension, left bending, and right bending angles of C0-C1, C1-C2, C2-C3, C3-C4, C4-C5, C5-C6, C6-C7, and C7-T1 joints and the neck (C0-T1) during static and dynamic tasks (task conditions) were treated as dependent variables. As the ROM data of the neck and the cervical joints met the normality assumption, we performed multi-factor Analysis of Variance (ANOVA) tests wherein *helmet condition, sex,* and their interaction were independent variables and the *subject* was treated as a random block. All statistical tests were performed at 95% confidence level (α = 0.05) and post-hoc tests—Tukey HSD for the ANOVA test and Nemenyi test for the non-parametric test—were performed to evaluate the significance of each factor level.

3. Results

3.1. Helmet effect

3.1.1. Peak neck angle data and neutral posture

Friedman tests showed significant differences for the helmet conditions, where the helmet use increased neck flexion (static: p < 0.001; dynamic: p = 0.0853), but decreased neck extension (static: p = 0.0106; dynamic: p = 0.00320) (Table 2). When compared to the baseline condition, the Nemenyi test showed that the US-style helmet condition significantly increased peak angle for static neck flexion (static: p = 0.0146, 15.1%; dynamic: p > 0.05, 9.71%), but it did not significantly decreased neck extension (static: p > 0.05, 10.0%; dynamic: p > 0.05, 15.9%), while the European-style helmet did not show any significant increase for neck flexion (static: p > 0.05, 8.49%; dynamic: p > 0.05, 5.04%) or decrease for neck extension (static: p > 0.05, 2.26%; dynamic: p > 0.05, 3.73%). Particularly, the US-style helmet exhibited a larger increase in neck flexion (static: 6.09% and dynamic: 4.44%) and a greater reduction in neck extension (static: 7.91% and dynamic: 12.64%) than the European-style helmet. Though the helmet use was not significant for neck lateral bending tasks (Table 2), the use of US-style helmet led to a larger lateral bending angle (right: 5.95% and left: 7.85%) than the European-style helmet, particularly to the left side (1.90%) than the right side. In addition, helmet use also decreased flexion–extension neck neutral posture compared to the no-helmet condition (p > 0.05; US-style: 65%; European-style: 113%).

3.1.2. Neck ROM data

The US-style helmet reduced neck flexion–extension ROM by 4.56% (p > 0.05), while the European-style helmet had no effect. Conversely, lateral bending ROM increased by 3.90% with the US-style helmet and decreased by 2.94% with the European-style helmet. ANOVA results indicated helmet usage significantly changed lateral bending ROM, with Tukey HSD tests showing a significant difference between the US-style and European-style helmets (p = 0.0299).

3.1.3. Peak cervical intervertebral kinematic data

For static trials, the significant effects (p < 0.05) of the helmet use were observed mainly for all cervical joints except for the C2-C3 joint during static right bending and the C5-C6 and C7-T1 joints during static left bending. Helmet use was also significant for dynamic flexion and extension, except for C0-C1 to C2-C3 joints, and for dynamic left bending for C0-C1 to C3-C4 joints (Fig. 3). The C0-C1 joint contributed the most towards the total neck peak angles during both static (16.1% and 20.6% for neck flexion and extension, respectively) and dynamic (23.3% and 17.4% for neck flexion and extension, respectively) tasks, followed by C4-C5, C5-C6, and C6-C7 joints. Interestingly, the C0-C1 joint exhibited trivial contributions (lower than 10%) during both lateral bending motions (Fig. 3).

3.1.4. Cervical intervertebral ROM data

ANOVA tests revealed significant helmet effects on flexion–extension ROM for C6-C7 and C7-T1 joints and on lateral bending for C0-C1, C1-C2, C2-C3, and C7-T1 joints. The US-style helmet differed significantly from both no-helmet and European-style helmets for C2-C3 and C7-T1, while the European-style helmet differed significantly from both other conditions for C0-C1 and C1-C2 joints. To explore it further, we calculated the distribution ratio between the dependent joint coordinates (movement) with respect to their coupled independent joint coordinate (movement) (Table 4). We observed that the motions of the lower and mid-cervical joints (C2 to C7) were somewhat evenly distributed (motion ratio = 12.6), while the motion of the upper cervical joints was mainly carried by the C0-C1 joint (motion ratio = 31.9). The independent joint coordinates of C1-C2 and C7-T1 remain the same, irrespective of intersubject variations and movement types.
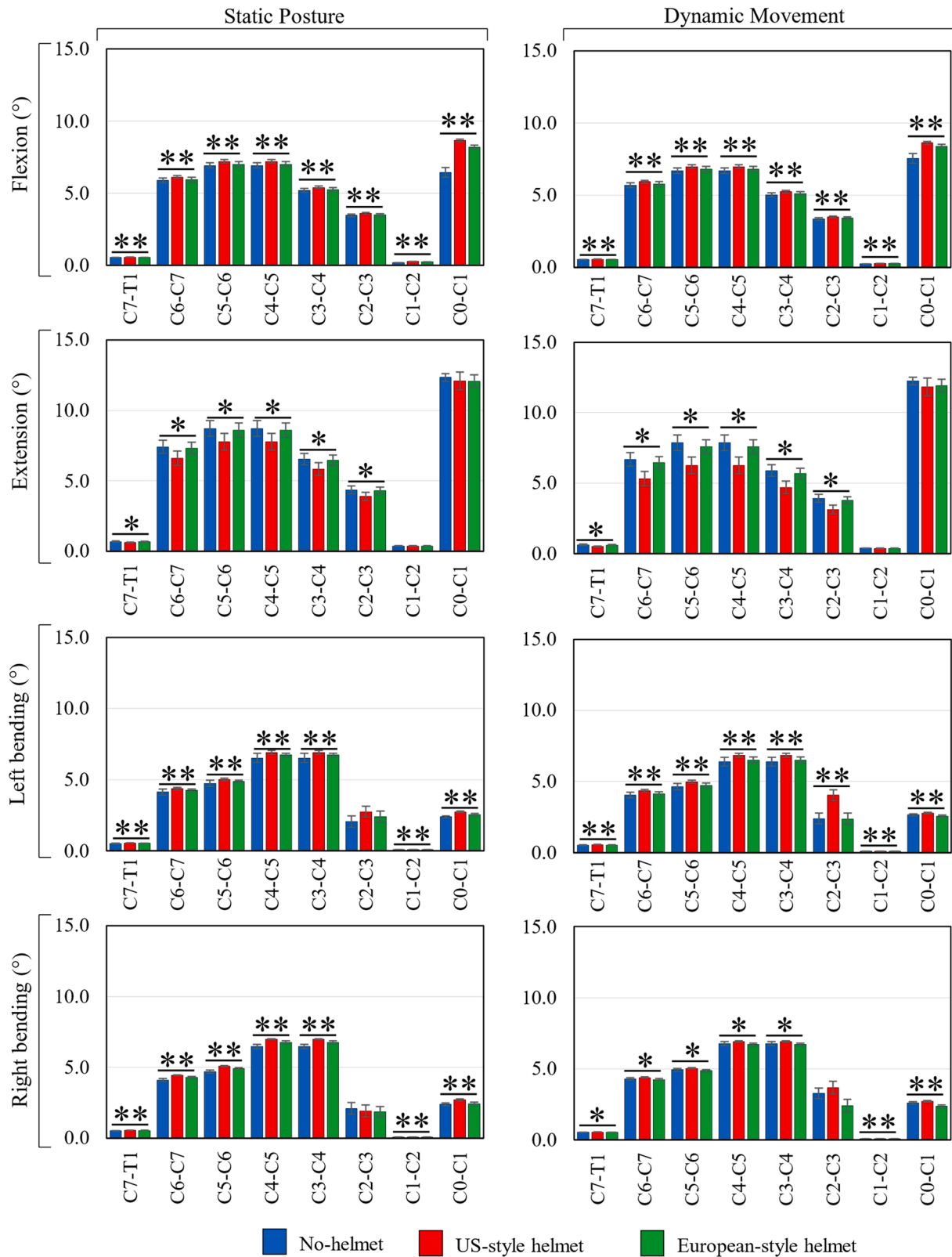
Fig. 3. The peak angles of individual intervertebral joints (C0-C1, C1-C2, C2-C3, C3-C4, C5-C6, and C7-T1) in extreme flexion, extension, and left and right lateral bending positions for all helmet conditions: no-helmet, US-style helmet, and European-style helmet. Asterisks are used to indicate whether helmet conditions presented significant differences for a joint (*: p-value < 0.05; **: p-value < 0.01).
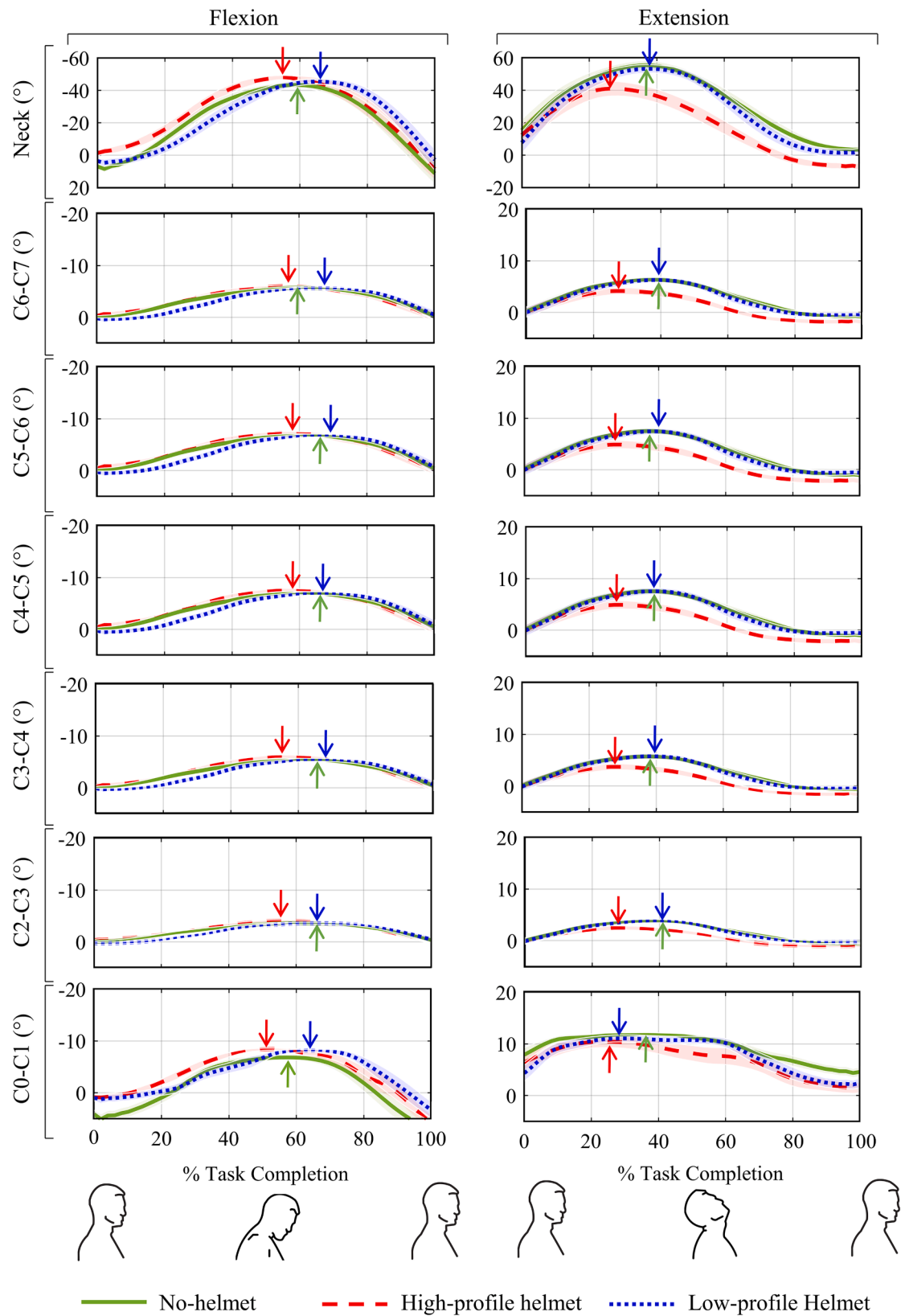
Fig. 4. Mean and standard error of flexion and extension movements of cervical spine joints for different helmet conditions. The C1-C2 and C7-T1 joints were not included as their movements were insignificant. The time-to-peak flexion and extension angles are indicated with arrow signs: red, blue, and green refer to corresponding time-to-peak angles for US-style helmet, European-style helmet, and no-helmet conditions, respectively. Figures in the x-axis representing the portion of the movement were inspired from (Anderst et al., 2015a). (For interpretation of the references to colour in this figure legend, the reader is referred to the web version of this article.)
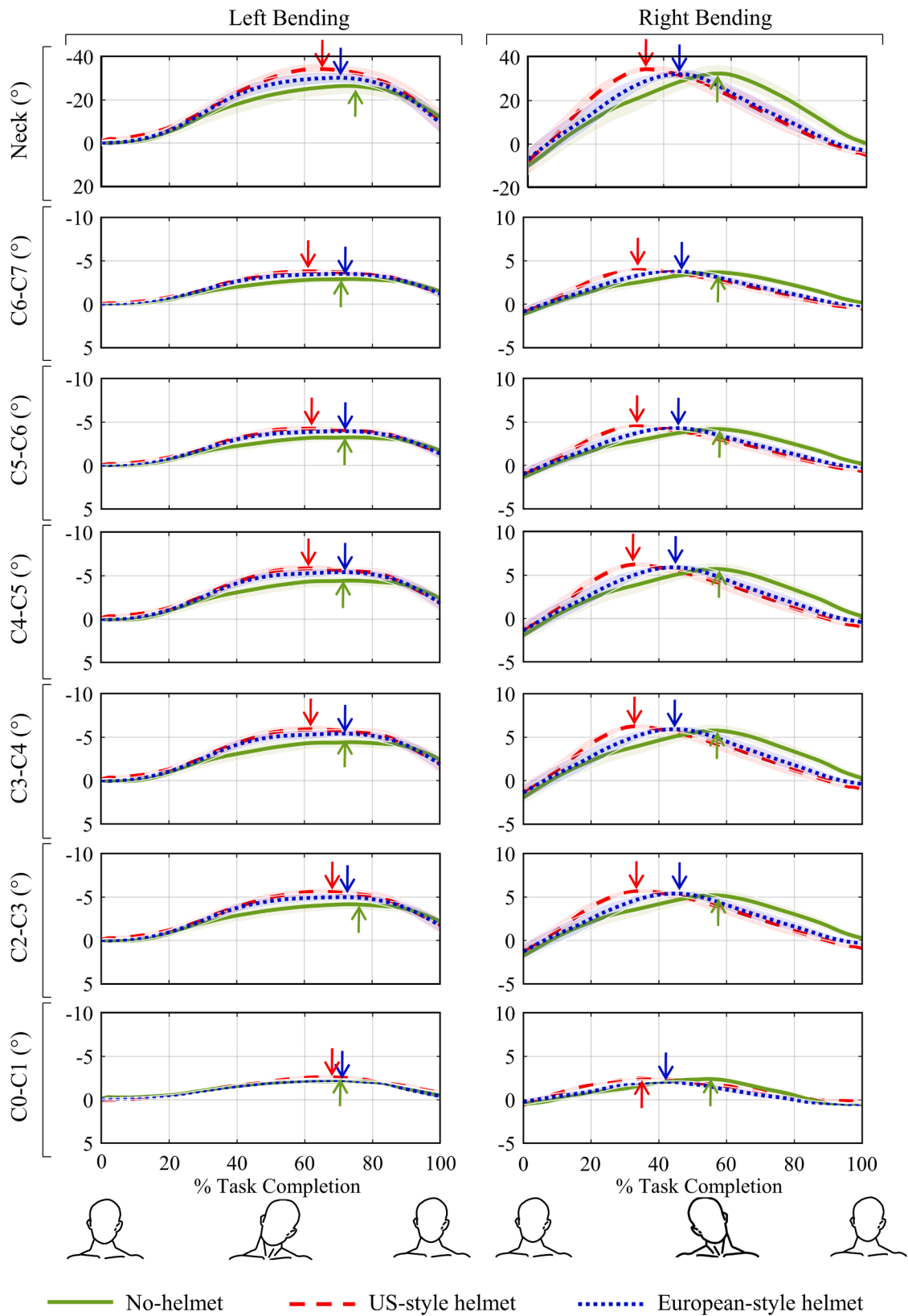
Fig. 5. Mean and standard error of left and right bending movements of cervical spine joints for different helmet conditions. The C1-C2 and C7-T1 joints were not included as their contributions in total neck movements were trivial. The time-to-peak flexion and extension angles are indicated with arrow signs: red, blue, and green refer to corresponding time-to-peak angle for US-style helmet, European-style helmet, and no-helmet conditions, respectively. Figures in the x-axis representing the portion of the movement were inspired from (Anderst et al., 2015a). (For interpretation of the references to colour in this figure legend, the reader is referred to the web version of this article.)

Table 3

Comparison of flexion–extension and lateral bending full range of motion for each cervical intervertebral joint and the total neck (C0-T1) between previous experimental studies.

| | | Cervical Intervertebral Joint | | | | | | | | |
		C0-C1	C1-C2	C2-C3	C3-C4	C4-C5	C5-C6	C6-C7	C7-T1	Neck Angle
Flexion-extension	Anderst et al. (2015)[1]	—-	15.6° ± 5.8°	12.7° ± 2.6°	17.1° ± 3.3°	19.5° ± 3.4°	19.7° ± 3.7°	15.8° ± 4.8°	8.3° ± 3.5°	119.0° ± 13.8°
	Zhou et al. (2020)[2]	6.3° ± 1.6°	13.7° ± 4.2°	9.5° ± 2.4°	14.9° ± 4.0°	19.4° ± 2.9°	17.1° ± 4.2°	12.3° ± 4.2°	4.1° ± 2.7°	94.5° ± 13.8°
	Cazzola et al. (2017)[3]	—-	—-	8.21°	12.4°	16.6°	16.6°	12.4°	7.34°	—-
	Nevins et al. (2014)[4]	—-	—-	—-	—-	—-	—-	—-	—-	92.3° ± 14.9°
	No helmet	19.8° ± 2.36°	15.5° ± 1.98°	7.90° ± 2.02°	11.9° ± 3.04°	15.4° ± 3.57°	15.1° ± 3.25°	12.7° ± 2.61°	6.67° ± 1.34°	103.5° ± 16.4°
	US-Style helmet	20.6° ± 3.40°	16.2° ± 2.83°	7.54° ± 1.75°	11.3° ± 2.64°	14.4° ± 3.27°	14.0° ± 3.10°	11.6° ± 2.56°	6.10° ± 1.33°	98.8° ± 14.2°
	European- helmet style	20.5° ± 2.2°	16.1° ± 2.70°	8.05° ± 1.81°	12.1° ± 2.75°	15.5° ± 3.27°	15.1° ± 3.00°	12.6° ± 2.40°	6.62° ± 1.24°	103.7° ± 12.9°
Lateral Bending	Anderst et al. (2015)[1]	—-	—-	—-	14.3° ± 2.8°	13.1° ± 3.2°	12.3° ± 2.61°	14.5° ± 3.9°	5.6° ± 2.4°	83.9° ± 14.5°
	Zhou et al. (2020)[2]	1.9° ± 1.5°	7.6° ± 2.7°	11.3° ± 4.5°	12.4° ± 3.1°	9.8° ± 2.4°	10.0° ± 2.3°	10.6° ± 3.3°	5.0° ± 2.8°	60.5° ± 14.4°
	Cazzola et al. (2017)[3]	—-	—-	6.25°	10.9°	12.4°	17.1°	17.1°	6.25°	—-
	Ishii et al. (2006)[5]	1.9° ± 0.9°	1.6° ± 1.3°	3.7° ± 2.0°	3.5° ± 1.4°	3.3° ± 1.0°	4.3° ± 1.4°	5.7° ± 1.9°	4.1° ± 2.7°	—-
	No helmet	5.89° ± 0.98°	9.75° ± 7.65°	12.2° ± 1.71°	13.5° ± 2.04°	13.4° ± 1.92°	9.78° ± 1.38°	8.52° ± 1.14°	4.81° ± 0.62°	75.5° ± 12.5°
	US-Style helmet	5.98° ± 0.71°	10.9° ± 5.34°	13.0° ± 0.80°	14.2° ± 0.98°	14.1° ± 0.84°	10.2° ± 0.63°	8.92° ± 0.48°	5.06° ± 0.24°	78.5° ± 6.01°
	European- helmet style	5.16° ± 0.72°	7.01° ± 2.55°	12.3° ± 1.22°	13.5° ± 1.35°	13.4° ± 1.26°	9.75° ± 0.91°	8.52° ± 0.77°	4.83° ± 0.43°	73.3° ± 7.12°

[1] The total neck angle in Anderst et al. (2015) is defined as the angle between the head and the torso of the subjects.

[2] Zhou et al. (2020) defined the range of motion from the difference between local coordinate systems of anatomic landmarks from 3D vertebral models.

[3] Cazzola et al. (2017) ROM values were estimated by applying a moment of 2 Nm over C1-C2 level in the MASI model in flexion–extension and lateral bending directions.

[4] Nevins et al. (2014) measured C1 angle by the vector connecting the posterior and anterior tubercule and C2-C7 angles by the vector that originated at the geometric center and orthogonal to the line formed by the midpoints of the superior and inferior endplates.

[5] Ishii et al. (2006) measured lateral bending by converting the matrix of volume registration into the matrix representing relative motion with respect to the inferior adjacent vertebra.

3.1.5. Cervical intervertebral movement patterns

The flexion and extension movement patterns (Fig. 4) showed that subjects went into the peak flexion and extension positions, respectively, by about 2% and 5% faster (averaged across all joints) with the US-style helmet than the no-helmet condition. In contrast, the European-style helmet exhibited about 1% faster flexion and 3% slower extension movements across all joints than the no-helmet baseline. Similarly, lateral bending movements (Fig. 5) of the neck and all joints (except the C2-C3 joint) showed that subjects went into peak left and right bending positions, respectively, by 5% and 9% faster with the US-style helmet, followed by 4% and 7% faster with the European-style helmet, compared to the no-helmet baseline (see supplementary data).

3.2. Sex effect

Kruskall-Wallis tests showed that sex has a significant effect on all the neck peak static angles ($p < 0.002$) and for dynamic left bending neck angle ($p = 0.0219$). The ANOVA showed that sex is a significant factor for neck ROM during flexion–extension ($p < 0.001$), while it was significant for all joints and neck for lateral bending ROM ($p < 0.002$). Yet, females broadly exhibited greater peak angles than their counterparts for all the peak angle conditions. They also showed a more extended neck neutral angle for no-helmet condition, while a more flexed neutral angle with the usage of helmets (US-style helmet: 744%; European-style helmet: 2.29%) (Table 2).

4. Discussion

The present study investigated the effects of firefighter helmet on cervical intervertebral kinematics during static and dynamic neck flexion, extension, right, and left bending tasks. Results demonstrated that the helmet COM had more pronounced effects on the cervical intervertebral kinematics than the helmet mass, particularly during full flexion and extension positions. In full flexion position, despite being lighter (12.4%; 250 g) than the European-style helmet, US-style helmet exhibited more hyperflexion and quicker attainment of peak flexion angles. Particularly, the longer moment arm of the US-style helmet, when compared to its counterpart, in the superior direction (38.2% and 5.8 cm more superior) induced a larger rotational torques at each cervical joint and caused faster dynamic neck movements (see supplementary data). Likewise, despite having a lesser anterior COM location than the European-style helmet, the US-style helmet reached peak extension angle more rapidly. This can be attributed to its superior COM that yielded about 10% higher MOI at C0-C1 joint than those observed with European-style helmet. Similarly, though the COM of the US-style helmet was less offset in the left lateral direction than the European-style helmet, it increased the peak left and right bending angles by 4.51% (1.3°) and 7.07% (2.6°), respectively, because its superior COM caused about 17.4% (0.016 kg.m^2) higher MOI in the superior direction. Thus, our findings highlighted the importance of a low-profile (i.e., less superior COM) helmet in order to yield a greater neck range of motion to the users. Finally, we observed some sex-specific significant differences in neck peak angles which aligns well with a previous study (Pan et al., 2018) with comparatively higher peak angles for females, agreeing with our initial hypothesis.

Interestingly, our results revealed a greater contribution from C0-C1 joint and a trivial contribution from C1-C2 joint during both flexion–extension and lateral bending movements. However, previous

Table 4

Ratio between dependent and independent cervical intervertebral joint. The joint mobility of C6-C7 to C2-C3 joints is dependent on the C7-T1 joint, while C0-C1 is dependent on C1-C2 joint.

Degree of freedom (DoF)	Cervical Intervertebral Joints Ratio					
	C7-T1					C1-C2
	C6-C7	C5-C6	C4-C5	C3-C4	C2-C3	C0-C1
Flexion-extension	10.7	12.6	12.6	9.45	6.30	31.9
Lateral Bending	7.85	9.00	12.4	12.4	11.2	28.6

studies (Anderst et al., 2015; Ishii et al., 2006; Zhou et al., 2020) showed an equal contribution (~11°) from both C0-C1 and C1-C2 joints during neck flexion–extension movements. This discrepancy was owing to the fact that the MASI model divided the cervical spine into two independent segments: 1) upper cervical spine (C0-C2) spine with C1-C2 as an independent rotational DoF and 2) mid and lower cervical spine (C2-T1) with C7-T1 as an independent rotational DoF (Cazzola et al., 2017; Vasavada et al., 1998). The other cervical joints in each of these two segments have dependent rotational DoFs and their kinematics are estimated as a percentage of the total motion of their corresponding independent rotational DoFs. Consequently, this led to a greater contribution from C0-C1 joint and trivial movement in C1-C2 in the upper cervical spine, in addition to a very slight movement in C7-T1 joint in the mid-lower cervical spine.

Furthermore, our baseline OpenSim-derived ROM were within one standard deviation when compared with experimentally-measured data for both flexion–extension (−13% ~ 12%) and lateral bending (−10 % ~25 %) neck movements (Table 3). The variations between OpenSim-derived ROM data and experimentally-measured literature data can be attributed to several factors. The experimental studies by Anderst et al. (2015); Ishii et al. (2006); Zhou et al. (2020) considered both translational and rotational movements (six DoFs) of the cervical intervertebral joints and the intervertebral joint angles were directly measured between the adjacent vertebra's anatomical planes. In contrast, existing OpenSim neck models employ three rotational DoFs and calculate the cervical intervertebral joint kinematics on a fixed axis of rotation (Amevo et al., 1991). Previous studies reported that the neck ROM in both flexion–extension and lateral bending decreases with age and males having significantly lower ROM than females after their 30 s (Pan et al., 2018). Thus, our findings of reduced neck and cervical intervertebral mobility can be associated to the fact that our study subjects were comparatively older and bulkier (high BMI) than reported experimental studies.

This study has several limitations. First, the effects of helmet inertial properties on neck axial rotation were not evaluated. Second, we recruited and analyzed a limited number of subjects and two different versions of firefighter helmets. Third, a certain extent of variations in estimating the neck and cervical intervertebral angles can be associated to the OpenSim optimization routines of scaling and IK processes; these variations would be different if we used a different assumptions and modeling platform. Fourth, as existing OpenSim neck models do not include translational DoFs and measure intervertebral rotational kinematics based on experimental head-neck kinematics by employing a fixed proportion of the independent coordinates. These estimates of cervical intervertebral kinematics may differ from their experimental counterparts, observed using radiographic methods, such as dynamic X-ray and fluoroscopy (Anderst et al., 2015; Ishii et al., 2006; Zhou et al., 2020). In summary, the present study is a first-of-its-kind investigation on the influence of helmet inertial properties on the cervical intervertebral kinematics during both static and dynamic neck exertions. Our findings established the critical role played by the helmet COM in adversely affecting the cervical spinal mobility and acknowledged the placement of helmet COM near to C0-C1 joint (i.e., designing a low-profile helmet) in order to reduce potential neck injuries during prolonged wear.

CRediT authorship contribution statement

Gustavo M. Paulon: Writing – original draft, Formal analysis, Data curation, Conceptualization. **S. Sudeesh:** . **Leonardo H. Wei:** Data curation, Formal analysis, Investigation, Methodology, Validation, Writing – review & editing. **Suman K. Chowdhury:** Writing – review & editing, Supervision, Investigation, Funding acquisition, Conceptualization.

Declaration of competing interest

The authors declare that they have no known competing financial interests or personal relationships that could have appeared to influence the work reported in this paper.

Appendix A. Supplementary data

Supplementary data to this article can be found online at https://doi.org/10.1016/j.jbiomech.2024.112364.

References

Amevo, B., Worth, D., Bogduk, N., 1991. Instantaneous axes of rotation of the typical cervical motion segments: a study in normal volunteers. Clinical Biomechanics 6, 111–117.

Anderst, W.J., Donaldson III, W.F., Lee, J.Y., Kang, J.D., 2015. Three-dimensional intervertebral kinematics in the healthy young adult cervical spine during dynamic functional loading. Journal of Biomechanics 48, 1286–1293.

Ariens, G.A., Van Mechelen, W., Bongers, P.M., Bouter, L.M., Van Der Wal, G., 2000. Physical risk factors for neck pain. Scandinavian Journal of Work, Environment & Health 7–19.

Barrett, J.M., Healey, L.A., Fischer, S.L., Callaghan, J.P., 2022a. Cervical spine motion requirements from night vision goggles may play a greater role in chronic neck pain than helmet mass properties. Human Factors 00187208221090689.

Barrett, J.M., McKinnon, C.D., Dickerson, C.R., Laing, A.C., Callaghan, J.P., 2022b. Posture and helmet configuration effects on joint reaction loads in the middle cervical spine. Aerospace Medicine and Human Performance 93, 458–466.

Barrett, J.M., Healey, L.A., McKinnon, C.D., Laing, A.C., Dickerson, C.R., Fischer, S.L., Callaghan, J.P., 2023. Head supported mass, moment of inertia, neck loads and stability: A simulation study. Journal of Biomechanics 146, 111416.

Boschman, J.S., Frings-Dresen, M.H., Van Der Molen, H.F., 2015. Use of ergonomic measures related to musculoskeletal complaints among construction workers: a 2-year follow-up study. Safety and Health at Work 6, 90–96.

Campbell, R., Molis, J.L., 2022. Firefighter Injuries on the Fireground. National Fire Protection Association (NFPA).

Cazzola, D., Holsgrove, T.P., Preatoni, E., Gill, H.S., Trewartha, G., 2017. Cervical spine injuries: a whole-body musculoskeletal model for the analysis of spinal loading. PloS One 12, e0169329.

Christensen, S.W.M., Palsson, T.S., Krebs, H.J., Graven-Nielsen, T., Hirata, R.P., 2023. Prolonged slumped sitting causes neck pain and increased axioscapular muscle activity during a computer task in healthy participants–A randomized crossover study. Applied Ergonomics 110, 104020.

Diyana, M.A., Karmegam, K., Shamsul, B., Irniza, R., Vivien, H., Sivasankar, S., Syahira, M.P.A., Kulanthayan, K., 2019. Risk factors analysis: Work-related musculoskeletal disorders among male traffic policemen using high-powered motorcycles. International Journal of Industrial Ergonomics 74, 102863.

Echarri, J.J., Forriol, F., 2005. Influence of the type of load on the cervical spine: a study on Congolese bearers. The Spine Journal 5, 291–296.

GBD, 2019. Global Burden of Disease Study 2019 (GBD 2019) Results., in: Seattle, U.S.I.f. H.M.a.E.I., 2020. (Ed.).

Guidotti, T., 1992. Occupational repetitive strain injury. American Family Physician 45, 585–592.

Hanks, M.M., Sefton, J.M., Oliver, G.D., 2018. Neck kinematics and electromyography while wearing head supported mass during running. Aerospace Medicine and Human Performance 89, 9–13.

Hino, H., Abumi, K., Kanayama, M., Kaneda, K., 1999. Dynamic Motion Analysis of Normal and Unstable Cervical Spines Using Cineradiography: An. In Vivo: Study. Spine 24, 163–168.

Hirsch, C., Schajowicz, F., Galante, J., 1967. Structural changes in the cervical spine: a study on autopsy specimens in different age groups. Acta Orthopaedica Scandinavica 38, 1–77.

Ishii, T., Mukai, Y., Hosono, N., Sakaura, H., Fujii, R., Nakajima, Y., Tamura, S., Iwasaki, M., Yoshikawa, H., Sugamoto, K., 2006. Kinematics of the cervical spine in lateral bending: In vivo: Three-dimensional analysis. Spine 31, 155–160.

Kent, R., Forman, J., Bailey, A.M., Funk, J., Sherwood, C., Crandall, J., Arbogast, K.B., Myers, B.S., 2020. The biomechanics of concussive helmet-to-ground impacts in the National Football League. Journal of Biomechanics 99, 109551.

Kim, M.G., Kim, K.-S., Ryoo, J.-H., Yoo, S.-W., 2013. Relationship between occupational stress and work-related musculoskeletal disorders in Korean male firefighters. Annals of Occupational and Environmental Medicine 25, 1–7.

Mathys, R., Ferguson, S., 2012. Simulation of the effects of different pilot helmets on neck loading during air combat. Journal of Biomechanics 45, 2362–2367.

Mokhtarzadeh, H., Bagheri, S., 2023. Streamlining C3D File Processing and Visualization: A User-Friendly Approach Using Google Colab and Open-Source Python Packages.

Mortensen, J.D., Vasavada, A.N., Merryweather, A.S., 2018. The inclusion of hyoid muscles improve moment generating capacity and dynamic simulations in musculoskeletal models of the head and neck. PloS One 13, e0199912.

Newman, P., Riches, A., Mara, J., Spratford, W., 2022. The effect of helmet mass and aircraft acceleration on cervical spine loads during typical fast jet aircraft pilot head motions. Journal of Science and Medicine in Sport 25, 855–860.

Nimbarte, A.D., Sivak-Callcott, J.A., Zreiqat, M., Chapman, M., 2013. Neck postures and cervical spine loading among microsurgeons operating with loupes and headlamp. IIE Transactions on Occupational Ergonomics and Human Factors 1, 215–223.

Pan, F., Arshad, R., Zander, T., Reitmaier, S., Schroll, A., Schmidt, H., 2018. The effect of age and sex on the cervical range of motion–A systematic review and meta-analysis. Journal of Biomechanics 75, 13–27.

Panjabi, M.M., Crisco, J.J., Vasavada, A., Oda, T., Cholewicki, J., Nibu, K., Shin, E., 2001. Mechanical properties of the human cervical spine as shown by three-dimensional load–displacement curves. Spine 26, 2692–2700.

Park, H., Park, J., Lin, S.-H., Boorady, L.M., 2014. Assessment of Firefighters' needs for personal protective equipment. Fashion and Textiles 1, 1–13.

Peterson, G., Pihlström, N., 2021. Factors associated with neck and shoulder pain: a cross-sectional study among 16,000 adults in five county councils in Sweden. BMC Musculoskeletal Disorders 22, 1–9.

Stemper, B.D., Yoganandan, N., Pintar, F.A., Maiman, D.J., Meyer, M.A., DeRosia, J., Shender, B.S., Paskoff, G., 2008. Anatomical gender differences in cervical vertebrae of size-matched volunteers. Spine 33, E44–E49.

Torma-Krajewski, J., Steiner, L.J., Lewis, P., Gust, P., Johnson, K., 2006. Ergonomics and mining; charting a path to a safer workplace.

Valente, G., Crimi, G., Vanella, N., Schileo, E., Taddei, F., 2017. nmsBuilder: Freeware to create subject-specific musculoskeletal models for OpenSim. Computer Methods and Programs in Biomedicine 152, 85–92.

Van Dijke, G.H., Snijders, C., Roosch, E., Burgers, P., 1993. Analysis of biomechanical and ergonomic aspects of the cervical spine in F-16 flight situations. Journal of Biomechanics 26, 1017–1025.

Vasavada, A.N., Li, S., Delp, S.L., 1998. Influence of muscle morphometry and moment arms on the moment-generating capacity of human neck muscles. Spine 23, 412–422.

Vasavada, A.N., Danaraj, J., Siegmund, G.P., 2008. Head and neck anthropometry, vertebral geometry and neck strength in height-matched men and women. Journal of Biomechanics 41, 114–121.

Vicon, 2023. Plug-in Gait Reference Guide. Vicon Motion Systems.

Wang, S., Park, J., Wang, Y., 2021. Cross-cultural comparison of firefighters' perception of mobility and occupational injury risks associated with personal protective equipment. International Journal of Occupational Safety and Ergonomics 27, 664–672.

Zhou, C., Wang, H., Wang, C., Tsai, T.-Y., Yu, Y., Ostergaard, P., Li, G., Cha, T., 2020. Intervertebral range of motion characteristics of normal cervical spinal segments (C0–T1) during in vivo neck motions. Journal of Biomechanics 98, 109418.